Thin Solid Films, *200* (1991) 311–320
PREPARATION AND CHARACTERIZATION

AlN/GaN SUPERLATTICES GROWN BY GAS SOURCE MOLECULAR BEAM EPITAXY*

Z. SITAR, M. J. PAISLEY, B. YAN AND R. F. DAVIS
Department of Materials Science and Engineering, Box 7907, North Carolina State University, Raleigh, NC 27695-7907 (U.S.A.)
J. RUAN AND J. W. CHOYKE
Department of Physics, University of Pittsburgh, Pittsburgh, PA 15260 (U.S.A.)
(Received April 25, 1990; accepted December 17, 1990)

AlN/GaN superlattices with layer thicknesses between 0.5 and 20 nm have been grown. The substrates were α(6H)-SiC(0001) and Al_2O_3(0001) (sapphire). The growth was performed using a modified gas source molecular beam epitaxy (MBE) technique. Standard effusion cells were used as sources of aluminum and gallium, and a small, MBE-compatible, electron cyclotron resonance plasma source was used to activate nitrogen gas prior to deposition. Auger, X-ray, and transmission electron microscopy studies confirmed the existence of well-defined layers. High resolution electron microscopy revealed pseudomorphic behavior between the two materials for layers thinner than 6 nm. By contrast, completely relaxed individual layers of GaN and AlN with respect to each other were present for bilayer periods above 20 nm. Cathodoluminescence showed a shift in the emission peak of up to 0.7 eV. The observed emission energy shifts were used to estimate the band discontinuities.

1. INTRODUCTION

Commercialization of light-emitting optoelectronic devices in the previous decade stimulated considerable interest in those III–V nitrides which possess a direct energy gap in the UV region of the spectrum. A comprehensive review regarding the thin film and optoelectronic research in GaN prior to 1988 has recently been published[1]. Depositions of AlN and AlGaN have also been studied[2,3].

Band gap engineering in the range 3.4–6.2 eV can be achieved either by solid solutions or by superlattices of GaN and AlN. The latter are favored for several reasons. As has been shown for the GaAs/GaAlAs system[4–7], optoelectronic devices using multiple quantum well structures instead of heterostructures exhibit lower threshold current density, lower non-radiative recombination rate, narrower emission spectra and reduced sensitivity to temperature. The lattice parameter mismatch between AlN and GaN is only 2.5%, and thus layered structures of these

* Presented at the 17th International Conference on Metallurgical Coatings and 8th International Conference on Thin Films, San Diego, CA, U.S.A., April 2–6, 1990.

0040-6090/91/$3.50

two materials offer a way of producing high quality, low dislocation density GaN- and/or AlN-based materials and devices. To our knowledge, superlattices of these two materials have not been produced prior to this investigation. These are also the first semiconducting superlattices exhibiting a band discontinuity well above 1 eV. Khan *et al.*[8] reported the growth and optical properties of GaN single quantum wells sandwiched between an AlGaN ternary alloy. They observed the energy shifts in the order of 40 meV.

In the following sections we describe the procedures used to deposit and characterize the layered structures as well as detail the results and conclusions of this research.

2. EXPERIMENTAL PROCEDURES

The growth system was a modified Perkin–Elmer 430 molecular beam epitaxy (MBE) system. Standard effusion cells were used for the evaporation of gallium and aluminum, while the nitrogen was activated in a small, MBE-compatible, electron cyclotron resonance plasma source[9].

The growth studies were conducted on (0001)-oriented α-SiC (6H polytype) and (0001)-oriented epitaxial quality sapphire substrates, both of which have a hexagonal structure. All substrates were chemically cleaned and thermally desorbed in the vacuum at 900 °C prior to the introduction in the growth chamber. All superlattices were grown under the same conditions, which are summarized in Table I.

TABLE I
GROWTH CONDITIONS

Nitrogen pressure	1×10^{-4} Torr
Nitrogen flow rate	4–5 standard $cm^3\ min^{-1}$
Microwave power	50 W
Nitrogen ion current density at the substrate	150–200 $\mu A\ cm^{-2}$
Substrate temperature	600 °C
Growth rates	
GaN	$\approx$ 2.5 nm min^{-1}
AlN	$\approx$ 1.6 nm min^{-1}
GaN buffer layer thickness	140 nm
Period thickness	1.5–40 nm
Number of periods	20–200
Total growth time	6–7 h

Scanning Auger microprobe (JEOL JAMP-30) analysis was used to determine the presence of impurities and the nominal compositions of the AlN and GaN layers. The superlattices were subsequently analyzed by X-ray diffractometry using Cu Kβ radiation to determine layer period and the crystalline quality of the films. Transmission electron microscopy (TEM) (Hitachi H-800) and high resolution electron microscopy (JEOL 200CX) were used for further analysis. Cross-sectional TEM specimens were prepared using standard techniques[10]. The luminescent properties of the samples grown on α(6H)-SiC were examined by cathodolumines-

cence. The spectra were taken at 77 K in the wavelength range 200–800 nm using an excitation electron beam energy of 7 KeV.

3. EXPERIMENTAL RESULTS

3.1. Chemical analysis

Figure 1 shows an Auger depth profile taken from a sample with 20 AlN/GaN double layers. The layers of each material were 10 nm thick. The profile indicates well-defined layers. The spectra indicate nominal AlN and GaN compositions and some mixing of gallium and aluminum in the AlN and GaN layers respectively. A small amount of interfacial mixing may be present; however, the Auger data exaggerate this phenomenon because of insufficient depth resolution. This resolution in the sputter Auger technique depends on the escape depth of the Auger electrons (about 5 nm) and the depth resolution of the sputtering process (also about 5 nm). For both, the reason was that the instrument's depth resolution in this study was in the same range as the layer thickness. The fact that the Auger depth profiling exaggerates interlayer mixing for very thin layers can be proven by examination of the TEM results (see below), which show well-defined layers even at a thickness of only 2 monolayers.

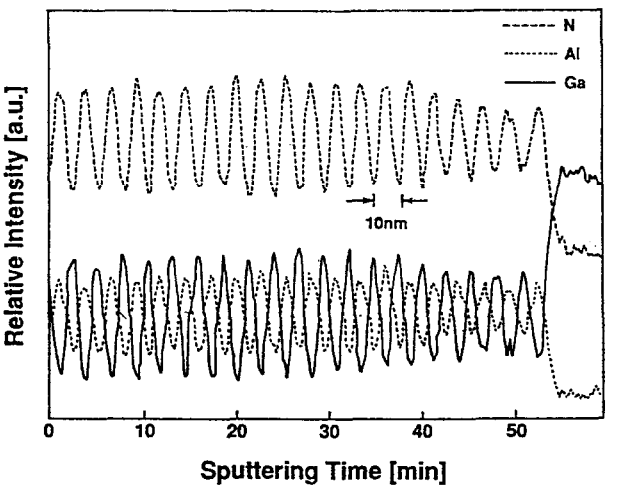

Fig. 1. Auger depth profile taken from a sample with 20 AlN/GaN double layers. The layers of each material were 10 nm thick.

3.2. Structural and microstructural analyses

3.2.1. X-ray analysis

Figures 2(a)–2(c) show the evolution of the diffraction peaks as a function of decreasing AlN/GaN bilayer periodicity P, which is given as

$$P = t_{AlN} + t_{GaN} \tag{1}$$

where t_{AlN} and t_{GaN} are the respective thicknesses of the individual layers of AlN and

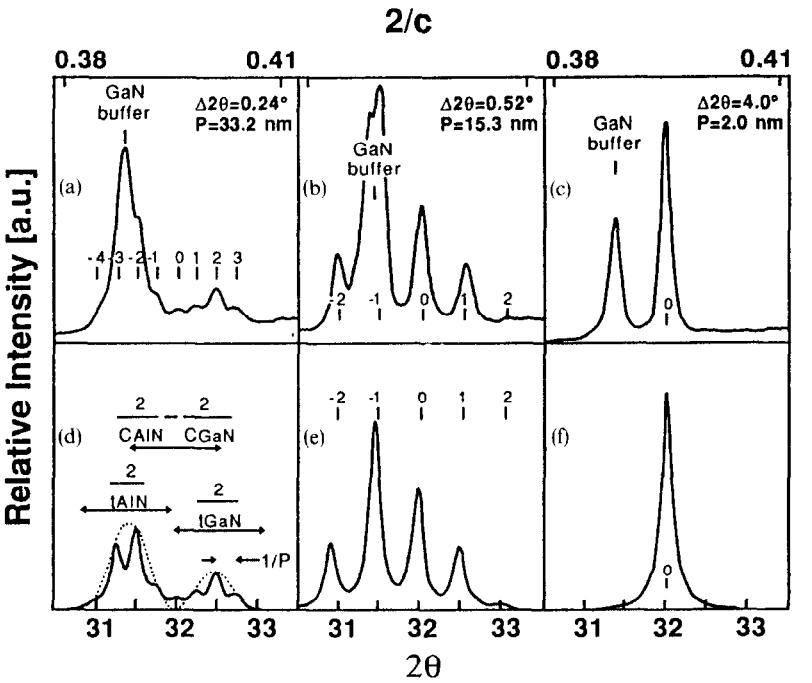

Fig. 2. (a)–(c) X-ray diffraction spectra of the samples with different periodicities. Each pattern is characterized by the (0002) peak from the GaN buffer layer (marked by "GaN buffer") and a zero-order peak from AlN/GaN layers at $2\theta = 32°$ (marked by "0") with satellite peaks around it. An angular spacing $\Delta(2\theta)$ of satellite peaks and a calculated bilayer period P is given for each spectrum. (d)–(f) Diffraction spectra after the subtraction of the GaN buffer layer peak and the overall background. (d) illustrates the use of the spectra for the determination of different parameters (see text).

GaN. Each spectrum shows the (0002) diffraction peak from the GaN buffer layer, the zero-order superlattice peak (marked "0") which represents the average vertical lattice parameter of the superlattice and the associated satellite peaks (marked from -4 to 3). The fact that the GaN and the zeroth-order superlattice peaks do not coincide shows that the superlattices are sufficiently thick to be structurally independent of the GaN buffer layer. As such, the lattice constant in the structure is characteristic of the superlattice rather than the substrate. The biaxial strain is shared between the GaN and the AlN layers, as the GaN layers are biaxially compressed and the AlN layers are biaxially dilated.

Since the buffer layer peak is superimposed on the superlattice peaks, it makes the diffraction from the superlattice unclear. As such, each spectrum in Figs. 2(a)–2(c) was fitted with a sum of lorentzian peaks followed by the subtraction of both the buffer layer peak and the overall background. This allows the evolution of the peaks with the change in superlattice period to be more easily observed. The resulting spectra are shown in Figs. 2(d)–2(f). In this set of spectra, the X-ray intensities are plotted as a function of $2/c$, where c is the lattice parameter perpendicular to the superlattice. This is convenient for measuring the parameters P, t_{AlN}, t_{GaN}, c_{GaN}, and c_{AlN} directly from the spectra. A representative diffraction spectrum having marked

parameters characteristic of a superlattice produced in this study is shown in Fig. 2(d).

Figure 2(d) shows two almost completely separated sets of superlattice peaks, each of which represents one of the two materials. The center of the GaN envelope coincides with the GaN buffer layer peak. This indicates that both have the same vertical lattice spacings. Since the center of the AlN envelope also appears at the same angular position as one would expect for the (0002) peak of bulk AlN, this indicates that individual layers at this period have unchanged vertical lattice parameters and thus are relaxed with respect to each other.

As the period decreases, the positions of the envelopes change. This is believed to be related to the biaxial lattice distortion due to elastic strain. In Fig. 2(e) both sets of peaks begin to overlap, and the exact positions of the two envelopes become less obvious. As one moves toward even shorter periods the two envelopes can no longer be resolved. As a consequence of shorter periods the number of observable satellite peaks decreases. Figure 2(f), which represents the diffraction spectrum of a superlattice with $P = 2$ nm, shows only the zero-order superlattice peak which is located approximately midway between the expected peaks for pure AlN and pure GaN. The peak corresponds to an interplanar spacing of 0.252 nm, which is intermediate between the spacings of the (0002) planes of AlN (0.249 nm) and GaN (0.258 nm) and represents the average spacing of the (0002) planes in the superlattice. Satellite peaks for this sample are out of the range of the scan, and are expected to be at about 28° and about 36°. As noted above, TEM results show a well-defined layered structure; thus, there is no reason to believe that this peak arises from the homogeneous mixing of the two materials.

According to the diffraction results, the transition between the relaxed and strained structures occurs at a layer thickness between 6 and 8 nm. This is in good agreement with the calculated value of 7.5 nm as the critical thickness using the method of Matthews and Blakeslee[11]. In order to determine more accurately the critical thickness, the reflections from the planes with mixed indices (for example $10\bar{1}1$)) should be studied.

3.2.2. Transmission electron microscopy

The periodicities calculated from the X-ray spectra were confirmed by the TEM images. Discrepancies between the two methods were found to be less than 5%.

Figure 3 shows a TEM image of 20 nm thick layers of AlN and GaN grown on α(6H)-SiC(0001). GaN layers are dark and those of AlN are light. Layers are well defined and have few structural defects. The $(01\bar{1}0)$ diffraction pattern (also shown), taken from the layered structure, confirms the monocrystalline nature of the film.

By contrast, structures grown on sapphire showed a columnar structure with slight misorientation. However, layers of the two materials within individual crystallites are well defined, and no misfit dislocations or other defects have been found for layers thinner than 7 nm. Even the structure containing 0.5 nm thick AlN layers (2 monolayers) and 1 nm thick GaN layers (4 monolayers), shown in Fig. 4, exhibits very good compositional contrast.

3.3. Optical characterization

The band gap difference between AlN and GaN is 2.8 eV. Thus layers of these

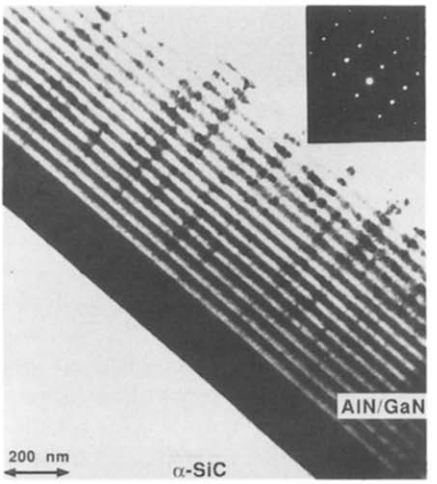

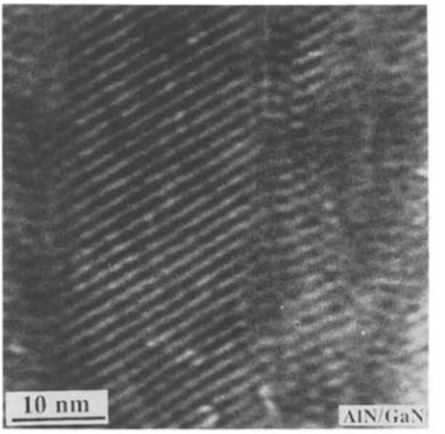

Fig. 3. AlN/GaN superlattices grown on α(6H)-SiC. The thickness of the individual layers is 20 nm. An electron diffraction pattern of this superlattice (zone axis $(01\bar{1}0)$), which confirms the crystalline quality, is also shown.

Fig. 4. TEM image of AlN/GaN superlattice grown on sapphire. The dark areas represent GaN and the light areas AlN. The thicknesses of AlN and GaN layers are 0.5 nm and 1 nm respectively.

two materials produce band discontinuities almost one order of magnitude larger than are achieved in AlGaAs or InGaAs systems. As such, AlN/GaN superlattices may provide some interesting insights regarding the behavior of electrons and holes. For example, they have the potential of providing several well-separated confined electronic states.

Two different cases were examined: (1) the emission energy shift as a function of the layer thickness with the thicknesses of the GaN and AlN layers maintained equal (*i.e.* $t_{AlN} = t_{GaN} = P/2$) and (2) the emission energy shift as a function of the barrier (AlN) thickness, while the well (GaN) thickness was maintained constant at 1 nm.

The allowed energy bands for the electrons in the conduction band and for the holes in the valence band in the superlattice were calculated using a one-dimensional Krönig–Penney model (see, for example, ref. 12). According to this model an electron or a hole can occupy a particular energy state in the superlattice only if the following is true:

$$1 \geq \left| \cos\left\{\frac{t_1(2mE)^{1/2}}{\hbar}\right\}\cosh\left[\frac{t_2\{2m(V-E)\}^{1/2}}{\hbar}\right] + \left(\frac{V}{E}-1\right)^{1/2}\left(\frac{V}{2E}-1\right)\sin\left\{\frac{t_1(2mE)^{1/2}}{\hbar}\right\}\sinh\left[\frac{t_2\{2m(V-E)\}^{1/2}}{\hbar}\right]\right|$$

In this expression is E the energy of the electrons (holes), V is the barrier height (band discontinuity), m is the effective mass of the carriers, $\hbar$ is Planck's constant divided by 2π, and t_1 and t_2 are the well and barrier widths respectively. Since there are no accepted values for the effective masses of the electrons and holes in either

AlN or GaN, the average values of the available data were used[13]. The effective mass of the electrons was taken as $0.2m_0$ and that of the holes as $0.8m_0$.

A conduction and valence band discontinuity was determined by iteration to provide the best fit to the transition energies observed by cathodoluminescence. The best fit was obtained when one-half of the total band gap discontinuity (1.4 eV) was assigned to the conduction band and one-half to the valence band. The total band gap discontinuity was calculated as the difference between the band gaps of AlN and GaN. Because of the lack of data on the mechanical properties of semiconducting nitrides, the effect of the biaxial strain on the band gap shift could not be included in the calculation, although it is expected to have a considerable influence on the band gap of both materials.

The shaded areas in Fig. 5(a) represent the lowest four calculated energy bands for the electrons in the conduction band and the holes in the valence band as a function of the individual layer thickness. The thicknesses of the AlN and GaN were considered equal in these calculations. The lowest transition energy in the superlattice at a particular layer thickness is obtained as the distance between the lower edge of the first energy band for the electrons and the upper edge of the first energy band for the holes. The arrows indicate the transitions in the structures with 1, 3, and 10 nm thick AlN and GaN layers. The different lengths of the arrows correspond to the emission energies observed by cathodoluminescence. The luminescence spectra for these three structures are shown in Fig. 5(b). The spectra show sharp and well-defined peaks with the energies above the band gap of GaN.

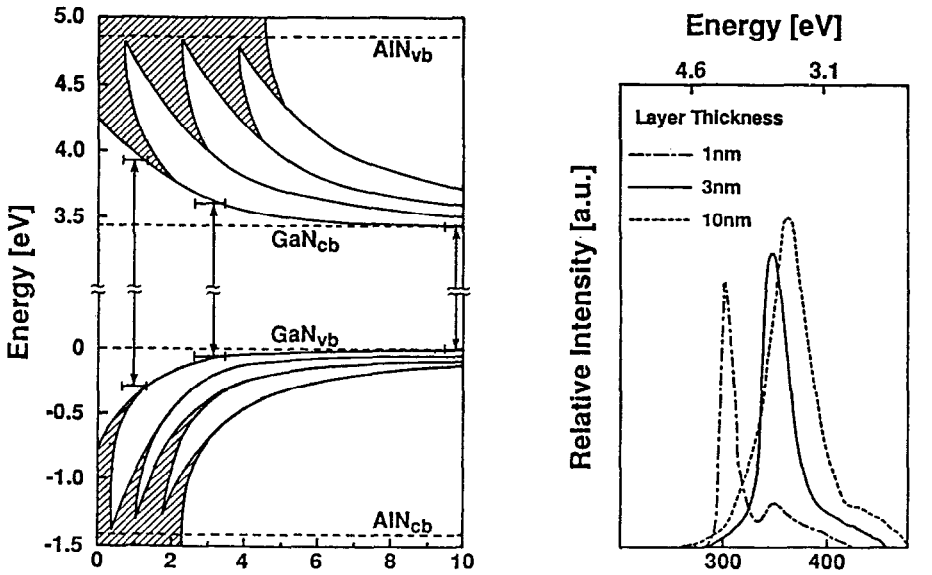

Fig. 5. (a) The lowest four calculated energy bands for the electrons in the conduction band and the holes in the valence band as a function of the individual layer thickness while the thicknesses of the AlN and GaN were kept equal. The arrows indicate the transitions in the structures with 1, 3, and 10 nm thick layers, whose cathodoluminescence spectra are shown in (b).

The width of the peaks increases with the layer thickness as the superlattice makes a transition from the pseudomorphic to a relaxed structure. The measured and calculated transition energies for these superlattices are collected in Table II.

TABLE II
CALCULATED AND MEASURED TRANSITION ENERGIES FOR DIFFERENT LAYER THICKNESSES

Layer thickness (nm)	$E_{calculated}$ (eV)	$E_{measured}$ (eV)	ΔE (meV)
1	4.29	4.11	180
3	3.64	3.47	170
10	3.42	3.42	≈ 0

The shaded areas in Fig. 6(a) represent the lowest two calculated energy bands for the electrons and the lowest three energy bands for holes as a function of the barrier width at a constant well width of 1 nm. The arrows again indicate the measured transition energy of a particular structure. The measured luminescence spectra for 0.5 nm and 1 nm thick barriers are shown in Fig. 6(b). The calculated and measured energies are summarized in Table III.

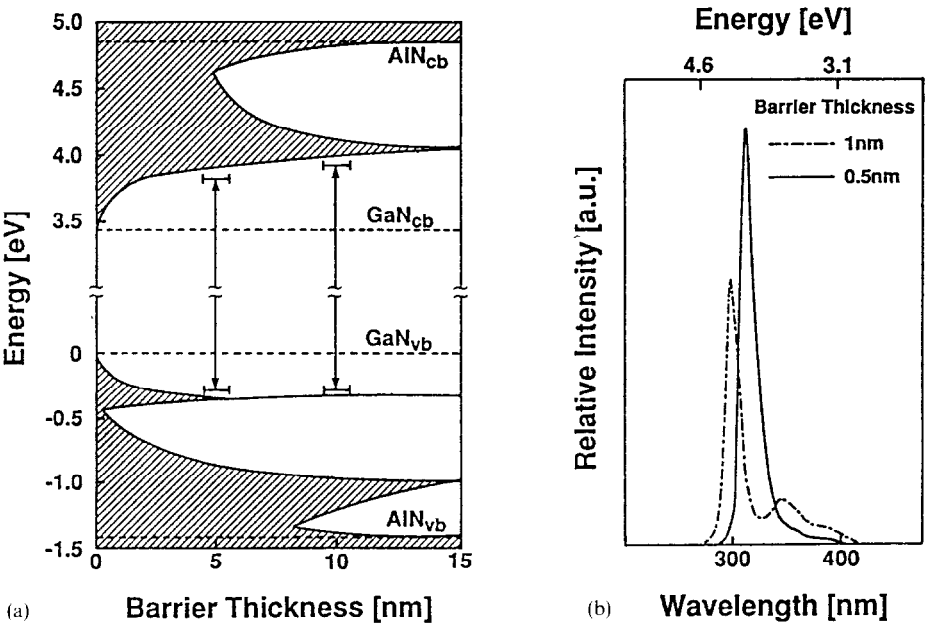

Fig. 6. (a) The lowest two energy bands for the electrons and the lowest three energy bands for the holes as a function of the barrier width at a constant well width of 1 nm. The arrows indicate the measured transition energies of particular structures. The measured luminescence spectra for 0.5 nm and 1 nm thick barriers are shown in (b).

TABLE III
CALCULATED AND MEASURED TRANSITION ENERGIES FOR DIFFERENT BARRIER THICKNESSES

Layer thickness (nm)	$E_{calculated}$ (eV)	$E_{measured}$ (eV)	ΔE (meV)
0.5	4.19	3.93	260
1.0	4.29	4.11	180

An examination of Tables II and III reveals the following information.

(1) The highest transition energy shift observed in this study was above 700 meV and occurred in the superlattice with 1 nm thick barriers and wells.

(2) The emission energy shift for the superlattice with 0.5 nm thick barriers was slightly lower than the previous value because of better coupling between adjacent wells (higher tunneling probability due to thinner barriers).

(3) There exists an energy offset between the calculated and measured values, which was in the range of experimental error for 10 nm thick layers and increased to 170 meV for thinner layers and even up to 260 meV for superlattices with the thinnest barriers.

The reasons for the observed offset can be several.

(1) There exists a possibility that the values for the effective masses used in the calculation are not accurate. For example, if the effective masses were larger, one would obtain lower theoretical values for the transition energies and, as such, a lower offset as well.

(2) The lattice mismatch between AlN and GaN produces strain, which induces band gap shift in both materials. This shift is expected to be rather high for the materials with 2% misfit (*i.e.* in the range of about 100 meV)[14].

(3) Interfacial mixing of aluminum in GaN and gallium in AlN in the monolayer scale could significantly change the transition energy in superlattices having individual layers only a few monolayers thick.

The offset for the moderately thin layers (1 and 3 nm) seems to be fairly constant (180 and 170 meV), which would not be the case if only an error in the effective masses were in question. The fact that the offset is negligible for thick layers (layers above the critical thickness, which are relaxed with respect to each other) and almost constant for the layers below the critical thickness (which are biaxially strained) implies a connection between the strain-induced band gap shift and the observed offset. As such, the luminescence data could be a rough indicator of whether a layered structure is pseudomorphic or not.

The offset for the superlattices with 2 monolayer thick barriers is even larger than that of the superlattices with moderately thin individual layers by an additional 90 meV. This jump, which could not be induced by the strain, is probably the consequence of interfacial mixing, which lowers the barrier height and, as a result, causes a decrease in the transition energy. A more sophisticated model, which would include band gap shift due to elastic strain and also assume 1 monolayer of interfacial mixing, is expected to give much better agreement between the experimental data and theory.

4. SUMMARY

Growth and characterization studies of AlN/GaN layered structures have been conducted using a modified gas source MBE technique. Layers as thin as 2 monolayers have been grown. X-ray and TEM results revealed strained material (no misfit dislocations at the interfaces) for layers thinner than 6 nm and a completely relaxed structure for layers thicker than 10 nm. Cathodoluminescence studies showed a transition energy shift as high as 700 meV due to the quantum size effect. There exists a constant offset of 170 meV between the experimental and calculated values. Since this offset is present only for the pseudomorphic structures, it has been related to the strain-induced band gap shift of the two materials.

ACKNOWLEDGMENTS

The authors wish to express their appreciation to Mr. Max Yoder (ONR) for his many helpful discussions and worthwhile suggestions. This work was sponsored by the SDIO/IST and managed by ONR under Contract N00014-86-K-0686.

REFERENCES

1 R. F. Davis, Z. Sitar, B. E. Williams, H. S. Kong, H. J. Kim, J. W. Palmour, J. A. Edmond, J. Ryu, J. T. Glass and C. H. Carter, Jr., *Mater. Sci. Eng. B*, *1* (1988) 77.
2 P. M. Dryburgh, *J. Cryst. Growth*, *94* (1989) 23.
3 Y. Koide, H. Itoh, M. R. H. Khan, K. Hiramatu, N. Sawaki and I. Akasaki, *J. Appl. Phys.*, *61* (1987) 4540.
4 W. T. Tsang, *Appl. Phys. Lett.*, *39* (1981) 786.
5 M. G. Burt, *Electron. Lett.*, *19* (1983) 210.
6 P. Davson, G. Duggan, H. I. Ralph and K. Woodbridge, *Superlattices Microstruct.*, *1* (1985) 173.
7 N. Holonyak, Jr., R. M. Kolbas, R. D. Dupuis and P. D. Dapkus, *IEEE J. Quantum Electron.*, *16* (1980) 170.
8 M. A. Khan, R. A. Skogman, J. M. Van Hove, S. K. Kutty and R. M. Kolbas, *Appl. Phys. Lett.*, *56* (1990) 1257.
9 Z. Sitar, M. J. Paisley, D. K. Smith and R. F. Davis, *Rev. Sci. Instrum.*, *61* (1990) 2407.
10 J. C. Bravman and R. Sinclair, *J. Electron Microsc. Tech.*, *1* (1987) 53.
11 J. W. Matthews and A. E. Blakeslee, *J. Cryst. Growth*, *27* (1974) 118.
12 R. L. Liboff, *Introductory Quantum Mechanics*, Holden-Day, San Francisco, CA, 1980.
13 *Landoldt-Börnstein New Series*, Vol. III/17d, Springer, Berlin, 1982.
14 N. G. Anderson, *Ph.D. Thesis*, North Carolina State University, Department of Electrical and Computer Engineering, 1988.